Role of cylindrical surface plasmons in enhanced transmission

Michael I. Haftel[a)]
Center for Computational Materials Science, Naval Research Laboratory, Washington, DC 20735-5343

Carl Schlockermann and Girsh Blumberg
Bell Laboratories, Lucent Technologies, Murray Hill, New Jersey 07974

(Received 23 December 2005; accepted 21 March 2006; published online 8 May 2006)

Utilizing normal mode analysis of Maxwell's equations and finite-difference-time-domain simulations we find extraordinary optical transmission in nanoarrays of insulating coaxial cylindrical rings embedded in metal films. As the rings become narrower we find transmission peaks at longer wavelengths, with the peak wavelength increasing indefinitely as the rings narrow. This behavior results from the excitation of cylindrical surface plasmon resonant modes on the cylindrical insulator-metal interfaces of the rings. These findings indicate that the excitation of cylindrical surface plasmons in these structures can produce propagating modes and enhanced transmission at wavelengths longer than those predicted previously. © *2006 American Institute of Physics*. [DOI: 10.1063/1.2201884]

Surface plasmons have been associated with "extraordinary optical transmission" (EOT) through nanoarrays of apertures in metal films ever since the demonstration of Ebbesen and co-workers.[1–3] This interpretation of EOT, with far-reaching implications for device development, is controversial. Other investigators suggest that shape resonances,[4,5] resonant coupling between array elements,[2,6,7] and diffractive effects[8] can account for EOT even without surface plasmons. Thus this role for surface plasmons is unresolved. In this letter we show that cylindrical surface plasmon (CSP) resonances, when excited in dielectric coaxial cylindrical apertures embedded in a metal film, can produce enhanced transmission at much longer wavelengths than by the effects considered heretofore.[1–8]

Our interest in coaxial structures stems from the theoretical investigations of Baida *et al.*,[9–12] who predicted enhanced transmission in finite-difference-time-domain (FDTD) simulations at very long wavelengths for coaxial ring (CR) nanoarrays. These predictions have been recently confirmed experimentally.[13] Transmission peaks from the ringed apertures in the optical range occur at wavelengths considerably redshifted from those of cylindrical apertures, *and the redshift increases as the ring is narrowed*. These previous investigators attribute the enhancements at long wavelengths to TE_1 guided modes of the individual coaxial rings[11] and not to the periodic structure. The present work confirms such a conclusion. Such modes can give rise to cylindrical surface plasmon excitations, i.e., "surface" waves, where here the surfaces are the cylindrical interfaces between the (real, not ideal) metal and the dielectric ring. This letter concentrates on how the enhancements, particularly the wavelengths at the peaks, depend on the ring geometry and how they arise out of the dielectric behavior of the real metal.

Cylindrical surface plasmons can be excited on cylindrical metal-dielectric interfaces by virtue of the negative dielectric constant of the metal. They can exist in the TE and/or TM mode with the strongest fields near the cylindrical interfaces.[14,15] The energy flow, which is concentrated near the interfaces, has a strong component up the aperture that can exit the apertures and efficiently couple to the far field. We diagram a "basic" coaxial ring structure that we consider in the present study (with variations in geometry) in Fig. 1, along with indications of the energy flow and field profile when cylindrical surface plasmons are excited.

We demonstrate the role of CSP's through this basic structure consisting of a square array of coaxial silica ($n=1.46$) rings with $d=555$ nm periodicity, with inner and outer radii $R_1=50$ nm and $R_2=100$ nm, embedded in an L

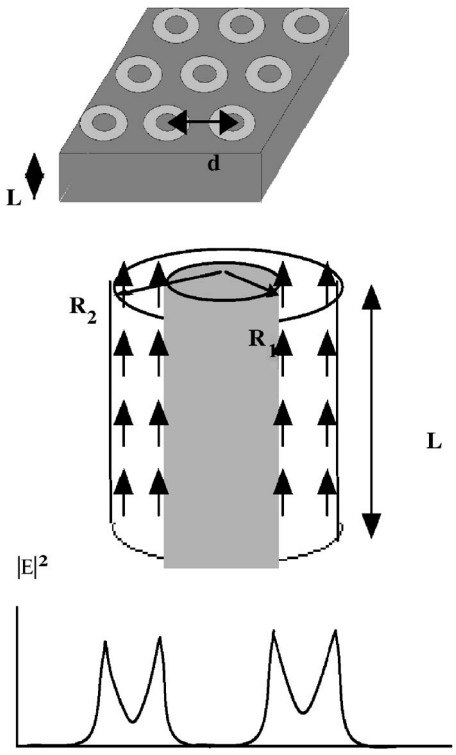

FIG. 1. The "basic" structure consisting of a square array of coaxial cylinders, spaced at $d=555$ nm, with inner Au cylinders with radii $R_1=50$ nm and an outer silica cylinder $R_2=100$ nm, in a Au film of thickness $L=290$ nm. The energy flow (arrows) and intensity profile when cylindrical surface plasmons are excited are qualitatively indicated.

[a)]Electronic mail: haftel@dave.nrl.navy.mil

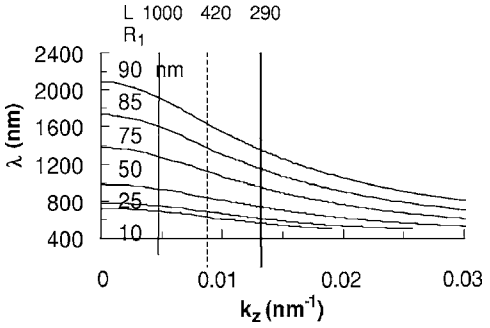

FIG. 2. The $n=1$ CSP dispersion curves for various R_1 values, with the outer radius $R_2=100$ nm. The vertical lines indicate the values of k_z corresponding to $k_z=\pi/L$, with L indicated in nm.

=290 nm thick Au film, all in a uniform silica medium. The incident light is linearly polarized and incident normal to the bottom of the Au film. We model the dielectric constant of Au with a form suggested by the Drude model,

$$\varepsilon_m(\omega)=\varepsilon_1-i\varepsilon_2/\omega\tau(1-i\omega\tau)+4\pi i\sigma'/\omega, \quad (1)$$

where ε_1, ε_2, τ, and σ' are fit to the experimental dielectric constant. Values of $\varepsilon_1=7.919$, $\sigma=0.0056$ fs^{-1} (we use Gaussian units), $\varepsilon_2=-14\,395.1016$, and $\tau=9.00$ fs yield a good fit to the experimental data[16] for $\lambda=550-2000$ nm.

We adapt previous approaches[14,15] to the coaxial cylinder normal mode problem to the present geometry, which is an infinitely long metal cylinder surrounded by a thin dielectric ring and then completely surrounded (to infinity) by the same metal, to derive $\omega_n(k_z)$ [or $\lambda_n(k_z)$], where n is the azimuthal state and k_z is the longitudinal wave number in the cylinder. This dispersion equation involves solving a matrix equation $\boldsymbol{M}a=0$, i.e., $\det(\boldsymbol{M})=0$, where $\boldsymbol{M}$ is the 8×8 matrix[15] derived from the boundary conditions for Maxwell's equations at the interfaces and a contains the TE and TM coefficients for the types of Bessel functions in each radial region. The matrix elements of $\boldsymbol{M}$ involve n, k_z, the Bessel functions at the interfaces, and the radial wave numbers k_m for the metal and k_d for the dielectric ring, where $k_i^2+k_z^2=\omega^2\varepsilon_i/c^2$.

Figure 2 gives $\lambda_1(k_z)$ for Au for six values of R_1. ($n=0$ modes are radially symmetric and cannot be excited by linearly polarized plane waves). We have used only the real part of ε_m, which dominates at optical frequencies and the near IR. The vertical lines correspond to the $k_zL=\pi$ values for various L. As the condition $k_zL=m\pi$ is the general condition for a longitudinal standing wave in the cylinder, the intersection of any of these lines (the vertical axis) with a given curve will give the wavelength for $m=1$ ($m=0$) at which the cylindrical mode is in resonance with the longitudinal mode, which we identify as a CSP resonance as the fields are largest near the interfaces because of the negative dielectric constant of the metal.

We see in Fig. 2 that for a given L the resonant wavelength increases rapidly as $R_1\rightarrow R_2=100$ nm, a counterintuitive result. This has far-reaching consequences in sensing and detecting devices where it is necessary to far exceed the diffraction limit. How does this behavior arise, and what limits apply? We now analyze the dispersion relation in the limit $R_1\rightarrow R_2$, $k_z=0$.

For $\lambda\geqslant500$ nm, $|\varepsilon_m|\gg|\varepsilon_d|$, thus $|k_m|\gg|k_d|$. Reasonably assuming $|k_m|R_1\gg1$, $k_d\Delta R\ll1$ (with $\Delta R=R_2-R_1$), $\Delta R/R_1\ll1$, we utilize Bessel function properties to derive (details elsewhere) a simple zero condition for $\det(\boldsymbol{M}_{\mathrm{TE1}})$, where $\boldsymbol{M}_{\mathrm{TE1}}$ is the 4×4 TE-TE part of $\boldsymbol{M}$ for $n=1$,

$$k_dR_1=(\omega/c)\sqrt{\varepsilon_d}R_1\approx[k_m(\omega)\Delta R/(2i+k_m(\omega)\Delta R)]^{1/2}. \quad (2)$$

If $|\varepsilon_m|$ is very large $k_dR_1=1$, which is the $\mathrm{TE}_{\perp}$ result for an ideal metal. For real negative ε_m, $k_m=(\omega/c)\sqrt{\varepsilon_m}$ is imaginary and the resonant frequency (ω_{res}) is real. Otherwise (e.g., a dielectric or finite conductor) ω_{res} is complex producing an evanescent mode. In the range $500\ \mathrm{nm}<\lambda<4000$ nm, $k_m\approx\mathrm{const}\approx0.04i$ nm^{-1} for Au, thus by Eq. (2), with $k_m\Delta R\ll1$, $\lambda\approx2\pi R_1/(|k_m|\Delta R)^{1/2}$, i.e., the cutoff wavelength increases indefinitely as $R_1\rightarrow R_2$. For longer wavelengths the imaginary part of ε_m, i.e., losses, dominate [Eq. (1)], and this enhancement effect starts to attenuate. For these frequencies, using Eqs. (1) and (2), the resonant frequency is $\sim\Delta R^{2/3}$ and is complex, which means a wider, weaker resonance.

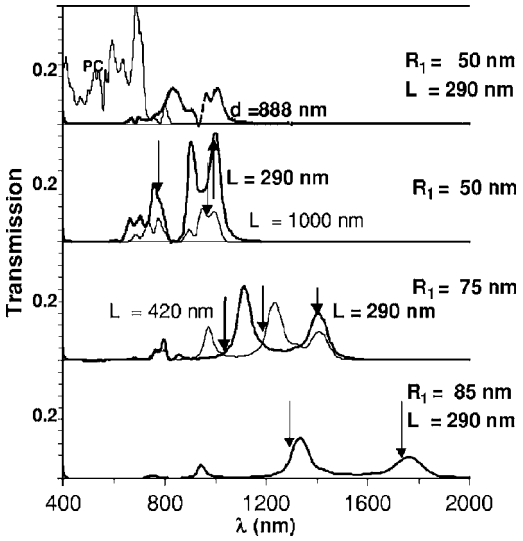

FIG. 3. Transmission spectra for various R_1 and L. The arrows indicate the theoretical $m=0$ and $m=1$ CSP resonance peaks. The top panel includes the cases of a perfectly conducting (PC) and a periodicity of $d=888$ nm (which has the same predicted resonance positions as the $R_1=50$ nm, $L=290$ nm case in the second panel).

We now confirm the role of cylindrical surface plasmons by FDTD simulations with the Naval Research Laboratory (NRL) high accuracy scattering and propagation (HASP) code[17,18] using the full dielectric constant [Eq. (1)]. The HASP code has been described elsewhere and its accuracy has been verified in exactly soluble models[19] and in reproducing experimental results.[18] We employ two-dimensional (2D) periodic boundary conditions parallel to the film and Mur absorbing boundary conditions in z. The spatial step is 6.9375 nm, and a typical time step is 0.02 fs. The incident plane wave has a period of 3.0 fs and Gaussian envelope of full width at half maximum (FWHM)=0.809 fs. We use the method of Gray and Kupka[20] to handle the frequency dependence of Eq. (1) in the FDTD algorithm.

Figure 3 gives the transmission spectra for various CR geometries. The top panel also gives results for a perfectly conducting (PC) metal and also results for periodicity $d=888$ nm. The theoretical $m=0$ and $m=1$ peaks, i.e., CSP peaks, as extracted from Fig. 1, are indicated by arrows. Typically the CSP peaks are redshifted slightly from the theoretical positions, but their movement and spacing with the ring width and cylinder length are well predicted, including

the dramatic redshifting as the ring narrows. Additional peaks appear because of surface plasmon resonances on the surfaces of the film. The insensitivity of the CSP peaks to the periodicity $d=888$ nm or $d=555$ nm also confirms that the cylindrical surface mechanism depends only on the geometry of the individual cylinders. The peaks due to CSP's are also dramatically redshifted from those of a PC indicating the importance of the finite negative ε of Au.

In a detailed study of the simulated fields we have confirmed the presence of CSP's in two other ways: (1) For the $m=0$ peaks the imaginary part of the Poynting vector is large and directed azimuthally in the CR—a characteristic of a CSP resonant mode. (2) At CSP resonant frequencies the components of the $\boldsymbol{E}$ and $\boldsymbol{H}$ fields peak at the dielectric-metal cylindrical interfaces (as in Fig. 1), characteristic of CSP surface waves. As the ring narrows, the CSP "wave functions" more efficiently overlap accounting for significant transmission despite the ever narrowing dielectric ring.

An additional question is how fast the transmission drops as the ring narrows, since necessarily the transmission is zero for $R_1=R_2$. For $R_1=75$ nm the transmitted energy represents 3.0 times and 4.7 times the incident energy on the dielectric rings at the $m=0$ and $m=1$ CSP peaks, respectively. For $R_1=85$ nm these ratios are 2.1 and 4.0, respectively, indicating a slight drop in efficiency, likely due to the increased role of losses at the longer wavelengths. Aside from losses, the drop in transmission appears to be no faster than the decrease in the exposed dielectric ring area.

In conclusion, we have shown theoretically and in simulations an extraordinary optical transmission produced by cylindrical surface plasmons in coaxial ring nanostructures. The wavelengths at which enhancements occur are maximized by narrowed rings and are well beyond those allowed classically or by other enhancement mechanisms. While this effect is eventually attenuated by losses in the far IR, one could exploit this feature in other regimes (IR, rf) by the development of metamaterials[21] with negative (effective) dielectric constant and low losses containing such CR structures. The properties we found should have a dramatic effect on device design and hopefully motivate experiments to fabricate (i.e., through ion beam milling, dry etch, electroplating, or related techniques) and explore these structures.

This work was partially supported by the Office of Naval Research. Computations were carried out under the Department of Defense High Performance Computation Modernization Project. Additional computing support was given by the Munich University of Applied Sciences.

[1] T. W. Ebbesen, H. J. Lezec, H. F. Ghaemi, T. Thio, and P. A. Wolff, Nature (London) **391**, 667 (1998).
[2] L. Martín-Moreno, F. J. García-Vidal, K. M. Pellerin, T. Thio, J. B. Pendry, and T. W. Ebbesen, Phys. Rev. Lett. **86**, 1114 (2001).
[3] W. L. Barnes, W. A. Murray, J. Dintinger, E. Devaux, and T. W. Ebbesen, Phys. Rev. Lett. **92**, 107401 (2004).
[4] K. J. Klein Koerkamp, S. Enoch, F. B. Segerink, N. F. van Hulst, and L. Kuipers, Phys. Rev. Lett. **92**, 183901 (2004).
[5] R. Gordon and A. G. Brolo, Phys. Rev. Lett. **92**, 037401 (2004).
[6] J. Bravo-Abad, F. J. García-Vidal, and L. Martín-Moreno, Phys. Rev. Lett. **93**, 227401 (2004).
[7] G. P. Wang, Y. Yi, and B. Wang, J. Phys.: Condens. Matter **15**, 8147 (2003).
[8] H. J. Lezec and T. Thio, Opt. Express **12**, 3629 (2004).
[9] F. I. Baida and D. van Labeke, Opt. Commun. **209**, 17 (2002); A. Moreau, G. Granet, F. I. Baida, and D. van Labeke, Opt. Express **11**, 1131 (2003).
[10] F. I. Baida and D. van Labeke, Phys. Rev. B **67**, 155314 (2003).
[11] F. I. Baida, D. van Labeke, and B. Guizai, Appl. Opt. **42**, 6811 (2003).
[12] F. I. Baida, D. van Labeke, G. Granet, A. Moreau, and A. Belkhir, Appl. Phys. B: Lasers Opt. **79**, 1 (2004).
[13] J. Salvi, M. Roussey, F. I. Baida, M.-P. Bernal, A. Mussot, T. Sylvestre, H. Maillotte, D. van Labeke, A. Perentes, I. Utke, C. Sandu, P. Hoffman, and B. Dwir, Opt. Lett. **30**, 1611 (2005).
[14] C. A. Pfeiffer, E. N. Economou, and K. L. Ngai, Phys. Rev. B **10**, 3038 (1974); S. S. Martinos and E. N. Economou, *ibid.* **28**, 3173 (1983).
[15] U. Schröter and A. Dereux, Phys. Rev. B **64**, 125420 (2001).
[16] P. B. Johnson and R. W. Christy, Phys. Rev. B **6**, 4370 (1972).
[17] W. Smith, W. Anderson, M. I. Haftel, E. Kuo, M. Rosen, and J. Uhlmann, Proc. SPIE **3696**, 250 (1999).
[18] D. Egorov, B. S. Dennis, G. Blumberg, and M. I. Haftel, Phys. Rev. B **70**, 033404 (2004).
[19] J. B. Cole, Comput. Phys. **12**, 82 (1998); IEEE Trans. Microwave Theory Tech. **45**, 991 (1997); S. A. Palkar, N. P. Ryde, M. R. Schure, N. Gupta, and J. B. Cole, Langmuir **14**, 3484 (1998).
[20] S. K. Gray and T. Kupka, Phys. Rev. B **68**, 045415 (2003).
[21] J. B. Pendry, L. Martin-Moreno, and F. J. Garcia-Vidal, Science **305**, 847 (2004).